

**The influence of the surface roughness, creep and relaxation on the performance of elastomeric liners for sustainable glass bottle closures**

Turan, Deniz; Poulis, Johannes A.

**DOI**

[10.1016/j.fpsl.2022.100840](https://doi.org/10.1016/j.fpsl.2022.100840)

**Publication date**

2022

**Document Version**

Final published version

**Published in**

Food Packaging and Shelf Life

**Citation (APA)**

Turan, D., & Poulis, J. A. (2022). The influence of the surface roughness, creep and relaxation on the performance of elastomeric liners for sustainable glass bottle closures. *Food Packaging and Shelf Life*, 32, Article 100840. <https://doi.org/10.1016/j.fpsl.2022.100840>

**Important note**

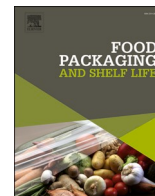
To cite this publication, please use the final published version (if applicable). Please check the document version above.

**Copyright**

Other than for strictly personal use, it is not permitted to download, forward or distribute the text or part of it, without the consent of the author(s) and/or copyright holder(s), unless the work is under an open content license such as Creative Commons.

**Takedown policy**

Please contact us and provide details if you believe this document breaches copyrights. We will remove access to the work immediately and investigate your claim.



# The influence of the surface roughness, creep and relaxation on the performance of elastomeric liners for sustainable glass bottle closures

Deniz Turan<sup>\*,1</sup>, Johannes A. Poulis

Structural Integrity Group, Faculty of Aerospace Engineering, Delft University of Technology, P.O. Box 5058, 2600 GB Delft, The Netherlands

## ARTICLE INFO

### Keywords:

Elastomer  
Seal  
Leakage  
Stress relaxation  
DMA  
Surface analysis

## ABSTRACT

Glass bottles having a metal closure are preferred for oxygen sensitive beverages e.g. beer. Using thinner closure which comprise polyvinyl chloride-free component is more sustainable. However, protecting the sealing performance as a result of metal closure thickness reduction is challenging. Here we show the relation between the leakage in beer bottles and surface roughness of three different thermoplastic elastomer seals. Compression relaxation and creep-recovery behavior of seals have been analyzed by using a dynamic mechanical analyzer. The results showed that metal downsizing was possible with Liner A (low density polyethylene (LDPE)/styrene-ethylene-butylene-styrene) and B (LDPE/ styrene-butadiene-styrene), but not with Liner C (high-density polyethylene/butyl rubber). Optimizing smaller surface topography parameters such as the surface roughness depth  $R_z$ , kurtosis  $S_{ku}$ , average void volume  $V_{vv}$ , arithmetic mean peak curvature  $S_{pc}$ , the density of surface peaks  $S_{pd}$  and higher peak material volume  $V_{mp}$ , peak material portion  $S_{mr}$  resulted in a better sealing performance. Liner C was found to show an increased leakage risk, since there was a high level of stress relaxation leading to a reduced sealing force. The sealing liner material with low relaxation, low elastic modulus and high creep recovery compliance was found to ensure better sealing when thinner metal closures are used.

## 1. Introduction

Crown caps (pry-off or twist) made of metal with an elastic sealing layer are used as closures for glass beverage bottles to ensure a leak-proof seal and to prevent carbon dioxide loss in case of carbonated drinks such as mineral water, beer, and so forth. Glass and metals provide a nearly absolute barrier to chemical and other environmental agents, but liner seals allow minimal levels of permeability acting as leakage points (Gagula et al. 2020; Paternoster et al. 2017). From a sustainability point of view, thinning of the metal closures is becoming a major challenge in this competitive market in order to remain cost-effective and more environmentally friendly by using less raw material and generating less waste and CO<sub>2</sub> emission per product. Previously, grade TH415 sheet metal (0.22 mm thick) was the most popular for pry-off caps. Recently, grade TH620 (0.18 mm thick) has become the main grade used for both pry-off and twist-off caps (Dey & Agrawal, 2016). Polyvinylchloride (PVC) containing sealing liners have been

widely used so far. However, PVC is not sustainable from an environmental perspective. It is very difficult to recycle PVC and disposal techniques for this material are not environmentally friendly (Moriga, Aoyama, & Tanaka, 2015). In order to keep up with the sealing performance of the caps of standard metal thickness with PVC liners, the reduced metal thickness caps sealed with innovative liner materials for glass bottle closure sealing is found to be a new challenge (Dey & Agrawal, 2016).

A liner is a piece of material that is positioned between the cap and the bottle. The liner of the beer bottle closure can be formed by an in-shell lining method in such a way that the finely rough surface is formed. The molten liner composition is bonded to the inner surface side of the bottle using a widely known thermoplastic or thermosetting adhesive, or by heat seal adhesion without using any particular adhesive (Koyama, Oda, Kikuchi, & Yamada, 1996). The crown cap is applied to the glass bottle using a crowner that exerts a straight downward force on the crown to crimp it onto the glass finish. The crowning head

*Abbreviations:*  $R_a$ , (arithmetic mean surface roughness);  $R_z$ , (surface roughness depth);  $S_a$ , (arithmetical mean height);  $S_q$ , (root mean square height);  $S_{sk}$ , (skewness);  $S_{ku}$ , (kurtosis);  $V_{vv}$ , (average void volume);  $V_{mp}$ , (peak material volume);  $S_{pc}$ , (arithmetic mean peak curvature);  $S_{mr}$ , (peak material portion);  $S_{pds}$  (the density of surface peaks); SEM, scanning electron microscopy; DMA, dynamic mechanical analyzer.

\* Corresponding author.

E-mail address: [d.kunter@tudelft.nl](mailto:d.kunter@tudelft.nl) (D. Turan).

<sup>1</sup> ORCID: 0000-0001-9480-8112

<https://doi.org/10.1016/j.fpsl.2022.100840>

Received 1 April 2021; Received in revised form 28 December 2021; Accepted 11 March 2022

Available online 16 March 2022

2214-2894/© 2022 The Author(s). Published by Elsevier Ltd. This is an open access article under the CC BY license (<http://creativecommons.org/licenses/by/4.0/>).

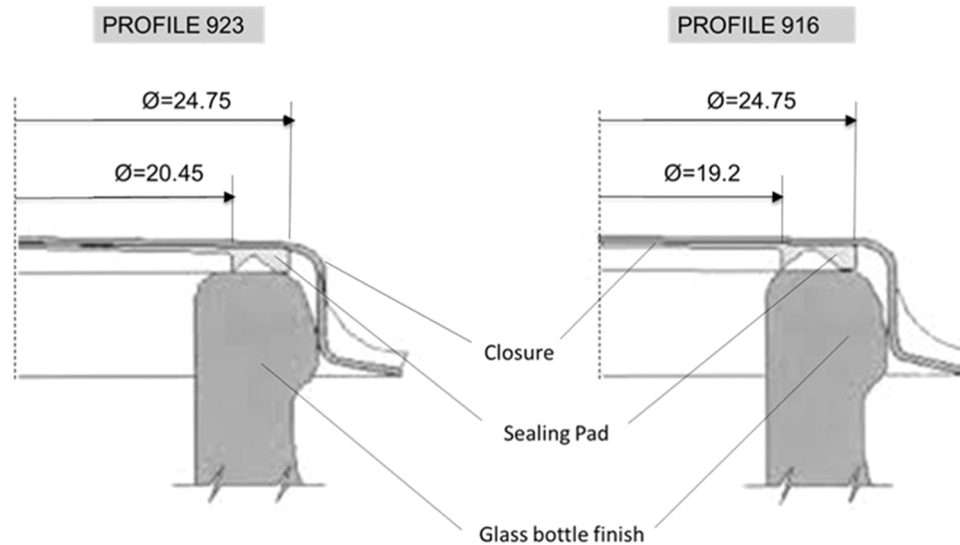


Fig. 1. Two different pry-off double lip profile.

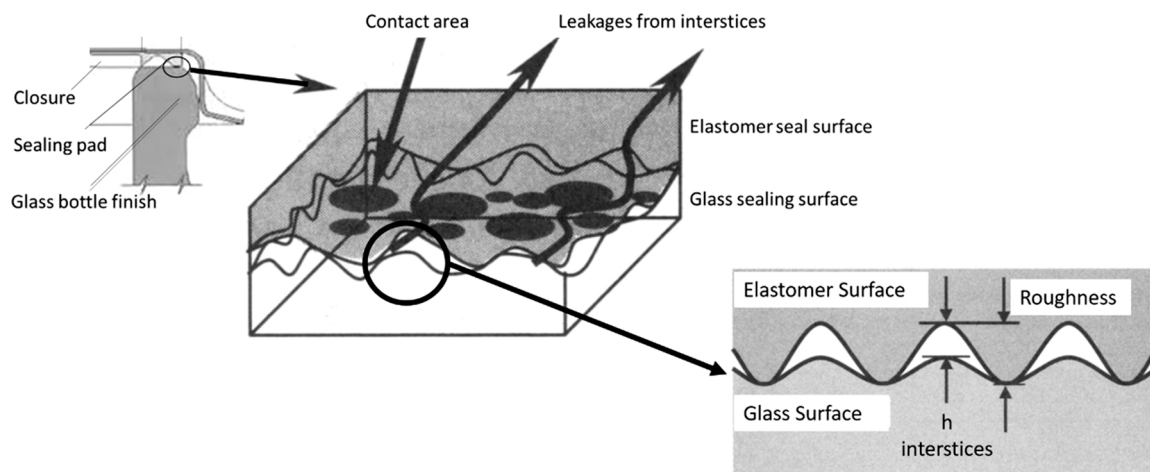


Fig. 2. Image of the contact state of sealing surface with surface roughness. Adapted from Otsuka et al., (2003).

compresses the crown liner to form a tight seal and bends the crown skirt downwards and inwards to lock it tightly underneath the locking ring of the glass on a pry-off finish (Robertson, 2016). A double or single closure lip may be provided on the liner's seal edge. In the case of a double closure lip, different profile types are available and the seal edge contacts the internal and external parts of the bottle neck (Fig. 1). One negative side effect of reduced thickness of the sheet metal downsizing is a reduction of sealing properties. With thinner sheet metal, there is a greater risk of loss of the leak-proof seal. For soft drinks this may lead to a carbon dioxide loss to below the limit permissible for a consumption beverage (Szymanski, 2011).

Recently, new PVC-free thermoplastic elastomer (TPE) liners have been introduced as a sealing pad (Grelle, Wolff, & Jaunich, 2017). A problem with elastomer seals is that there will always exist some surface roughness on the sealing surface due to the seal material or processing method. However, a suitable surface roughness at which no leakage occurs is not yet well defined. Previous studies showed that the sealing phenomena were related to the ratio of seal surface contact pressure / elastic modulus of the seal, determined by the compression ratio of seals. If the seal contact surface pressure is the same, the interstice  $h$  (leakage point) will decrease if the elastic modulus is small, and increase if large (Fig. 2). Thus in the case of elastomer seals, sealing cannot be expressed

only by the seal surface contact pressure because the critical compression ratio changes proportionately with the surface roughness (Otsuka, Okamura, Suetsugu, Ohta, & Ono, 2003). Therefore, studying the complex characteristics of microscopic surface topography, and comprehensively clarifying the influence mechanism of the surface topographic microstructures on sealing are of great significance to improve the quality of the sealing properties (Shi, Wang, Yan, Wang, & Dong, 2019). Moreover, in order to achieve an excellent sealing property, stress relaxation or creep deformation should preferably not occur in the contact area between the liner and the bottle finish. The material must have an appropriate elasticity when it undergoes deformation recovery (Sanchez-Gonzalez & Pérez-Terrazas, 2018). This allows the liner to properly align itself with the surface of the glass surface without being detached (Moriga et al. 2015). However, a study on sealing mechanisms focusing on the deformation of seal into rough sealing surfaces in relation to the effect of stress relaxation and creep phenomena has not been reported in literature yet.

In this study, we aimed to investigate the relation between the leakage and surface roughness of the elastomeric sealing materials including elastic deformation, stress relaxation and creep phenomena to understand how metal downsizing might allow TPE liners without leakage.

**Table 1**  
Properties of supplied thermoplastic elastomer (TPE) liners.

Sealing Compound	Shore Hardness	Melt Flow Index (dg/min)	Compression Set @ 23 °C (%)
Liner A	A 68	7	17
Liner B	A 88	30	30
Liner C	D 50	20	N/A

## 2. Materials and methods

### 2.1. Materials

The thermoplastic elastomer (TPE) liners are rubber-plastic blends supplied by Actega DS GmbH (Bremen, Germany), and were obtained in pellet form. The shore hardness (ASTM D 2240–05), melt flow index (ISO 1133:2005, 5 kg, 190 °C) and compression set (ASTM D 395, at room temperature) values of the different materials provided by the supplier are listed in Table 1. The hard phase of Liner A consists of a low density polyethylene (LDPE) and the soft phase of a styrene-ethylene-butylene-styrene (SEBS). Liner B is TPE-S (styrene butadiene copolymer) modified polyethylene (blend of LDPE and styrene-butadiene-styrene (SBS)). The hard phase of Liner C consists of a high-density polyethylene (HDPE) and the soft phase of a butyl rubber (IIR).

### 2.2. Sample preparation and characterization tests

Three different liners were molded into caps shells with three different metal thicknesses (0.22 mm, 0.20 mm and 0.18 mm) by using an in-shell lining machine from Sacmi Group (Imola, Italy) available in Actega DS GmbH (Bremen, Germany) in the form of a pry-off double lip profile 916. Automatic lining machines designed to extrude pellet-form material, cut it into single doses, and were inserted into aluminum screw caps as shown in Phase 1, Fig. 3). The liner is compression molded in Phase 2 according to a clearly defined profile (Phase 3). The cap's shells are heated by a low-frequency magnetic induction unit equipped with a cooling system so as to liquefy the internal paint which acts as adhesive primer between the liner and the cap. Extruder screw speed was 80 rpm and extrusion temperatures were 170 °C, 160 °C and 200 °C for Liner A, Liner B and Liner C, respectively.

The sealing performance of the liners at different metal thicknesses was evaluated. The leakage pressure of each metal closure profile sealed with three different liners for pasteurized bottles was measured by using an in-house leaking pressure instrument. For each liner, 40 bottles were closed with the same crimp molds dedicated for the closure with metal closure thicknesses of 0.22 mm, 0.20 mm and 0.18 mm. During the seal leaking pressure test method, the metal closure on the filled bottle is

pierced with a needle device, connected to a pressure generator and immersed into a small basin filled with tap water at room temperature. Through the needle device the pressure inside the bottle is increased with 3 bar/min. Once gas bubbles appear in the basin, the leaking pressure is recorded.

Parameters in the ISO 25178 standard were selected to explore the relationship between surface topography and interface characteristics (see Table 1A in Appendix for surface parameters) (Aver'Yanova, Bogomolov, & Poroshin, 2017). The 3D profilometer used in the experiment was the VR series 3D profilometer VR-5000, Keyence (Osaka, Japan) for surface parameters  $S_a$  (arithmetical mean height),  $S_q$  (root mean square height),  $S_{sk}$  (skewness),  $S_{ku}$  (kurtosis),  $V_{mp}$  (peak material volume),  $V_{vp}$  (average void volume),  $R_a$  (arithmetic mean surface roughness) and  $R_z$  (surface roughness depth). The measuring range was 206 mm × 104 mm, the measuring accuracy was 0.5 μm, and the imaging component was a 1 in. and 4-megapixel monochrome Complementary Metal Oxide Semiconductor (CMOS) camera (1 in. and 4 million pixels, Keyence, Osaka, Japan). A Keyence VK-9700 Laser Confocal microscope with x2.5 magnification (Keyence Corporation, Osaka, Japan) was used to perform surface profiles of closure lips for parameters  $S_{pc}$  (arithmetic mean peak curvature),  $S_{pd}$  (density of peaks) and  $S_{mr}$  (peak material portion). Five measurements were run independently for each sample. The characterization with scanning electron microscopy (SEM) was done by a JEOL JSM-7500 F (Tokyo, JAPAN) operated at an accelerating voltage of 5 kV and a probe current of approximately 10 μA. The liner surfaces were coated with a gold layer for 90 s at a coating thickness of 2 nm using a sputter coater (Quorum Q300T, East Sussex, UK) for enhanced conductivity to reduce static loading during the SEM experiments.

Stress relaxation and creep-recovery measurements were performed with a dynamic mechanical analyzer (DMA RSA-G2 Solids Analyzer, TA Instruments, USA) used in compression mode. A parallel plate fixture was used to clamp specimens, which were discs with a diameter of 8 mm and a uniform thicknesses of 2 mm. Disc shaped specimens were

**Table 2**  
Compound and injection molding parameters of thermoplastic elastomer (TPE) liners.

Parameters	Liner A	Liner B	Liner C
Processing temperature (°C)	175	160	205
Mixing time (min.)	2	2	2
Screw speed (rpm)	80	80	80
Barrel temperature (°C)	180	165	210
Mold temperature (°C)	40	30	45
Injection pressure (bar)	12	10	14
Holding time (sec.)	5	5	5

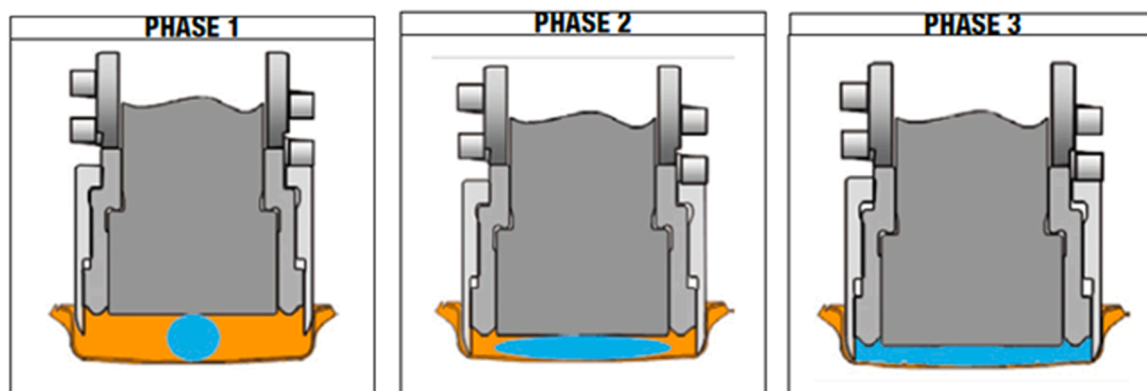


**Fig. 3.** The in-shell lining process for metal caps showing the three basic steps; Phase 1: placing individual pellets (blue color) into the cap shell (orange color), Phase 2: compression molding, Phase 3: forming the final profile shape. (For interpretation of the references to colour in this figure, the reader is referred to the web version of this article.)

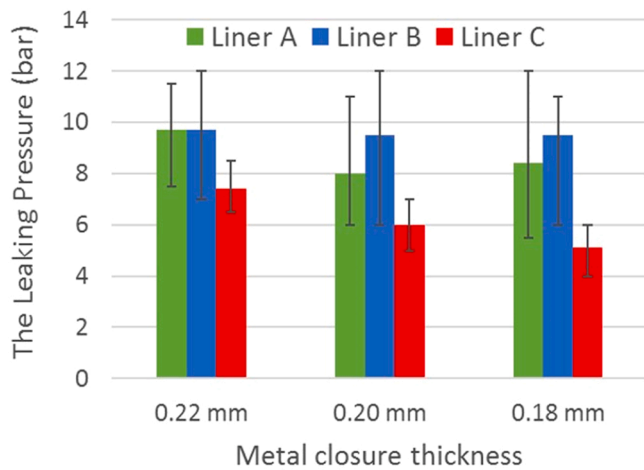


Fig. 4. The metal thickness downsizing effect on the leaking pressure of three different liners.

prepared by cutting them from injection molded samples according to ASTM D6147 - 97(2020). A vertical, co-rotating twin-screw micro-compounder (DSM Xplore 15 ml, Geleen, The Netherlands) and a micro 10 cc injection molding machine (DSM Xplore, Geleen, Netherlands) were used for melt mixing and injection molding, respectively. The compounding and injection molding parameters applied for the specimen production are listed in Table 2. The applied preload force was 1 N to prevent the sliding of the test specimens. The isothermal temperature was 25 °C. The stress relaxation tests were performed by

displacing the clamp position at a specified strain and measuring the stress decay as a function of time and temperature. The constant strain was set as 0.1%. The creep experiments were conducted in a similar manner to the stress relaxation. Strain (creep) was varied as a function of time and temperature and the stress was held constant. The input stress was set as 0.02 MPa. Strain sweeps were previously performed to ensure that the viscoelastic response was linear. The Young’s modulus of elasticity of the specimens was calculated from the slope of the linear portion of the stress-strain curve using the DMA data. All tests were done under a flowing air stream of dried air. Three specimens for each liner were used for stress relaxation and creep-recovery tests.

### 3. Results and discussion

The seal leaking pressure test was carried out in order to investigate the effect of metal thickness downsizing on the performance of liners and seal integrity. The range of leaking pressure of Liners A and B was between 6 and 12 bar and showed no significant differences with metal thickness downsizing. However, Liner C showed already a significantly lower mean leaking pressure than the other two liners at a metal thickness of 0.22 mm (Fig. 4) meaning that Liner C shows a lower quality of sealing performance. The sealing performance of Liner C showed a significant decrease with metal thickness downsizing to 0.18 mm.

The surface roughness parameters were studied to clarify the influence of the surface topography microstructures on the sealing performance. It is common practice in industry to consider some line roughness parameters, in particular  $R_a$  (arithmetic mean surface roughness) and  $R_z$  (surface roughness depth) as the main parameters considered when characterizing the quality of a product’s surface finish.

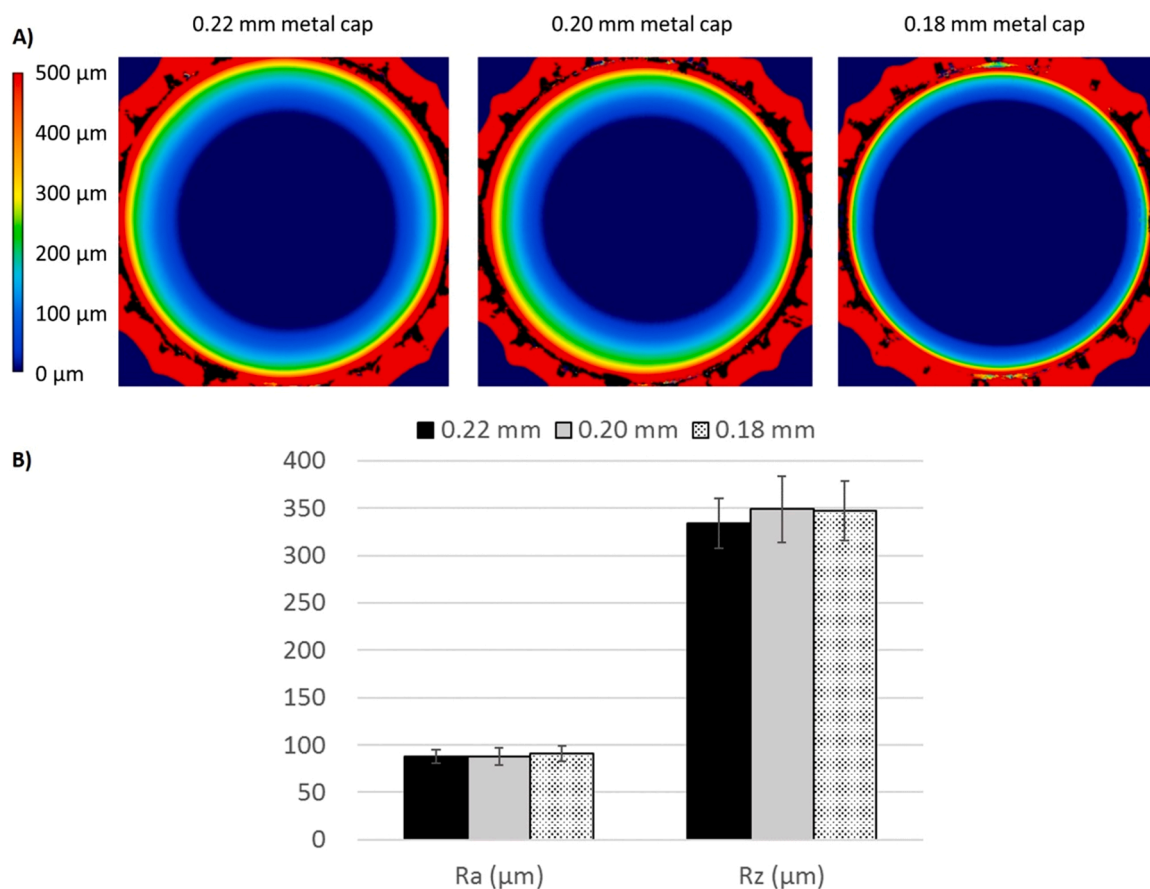
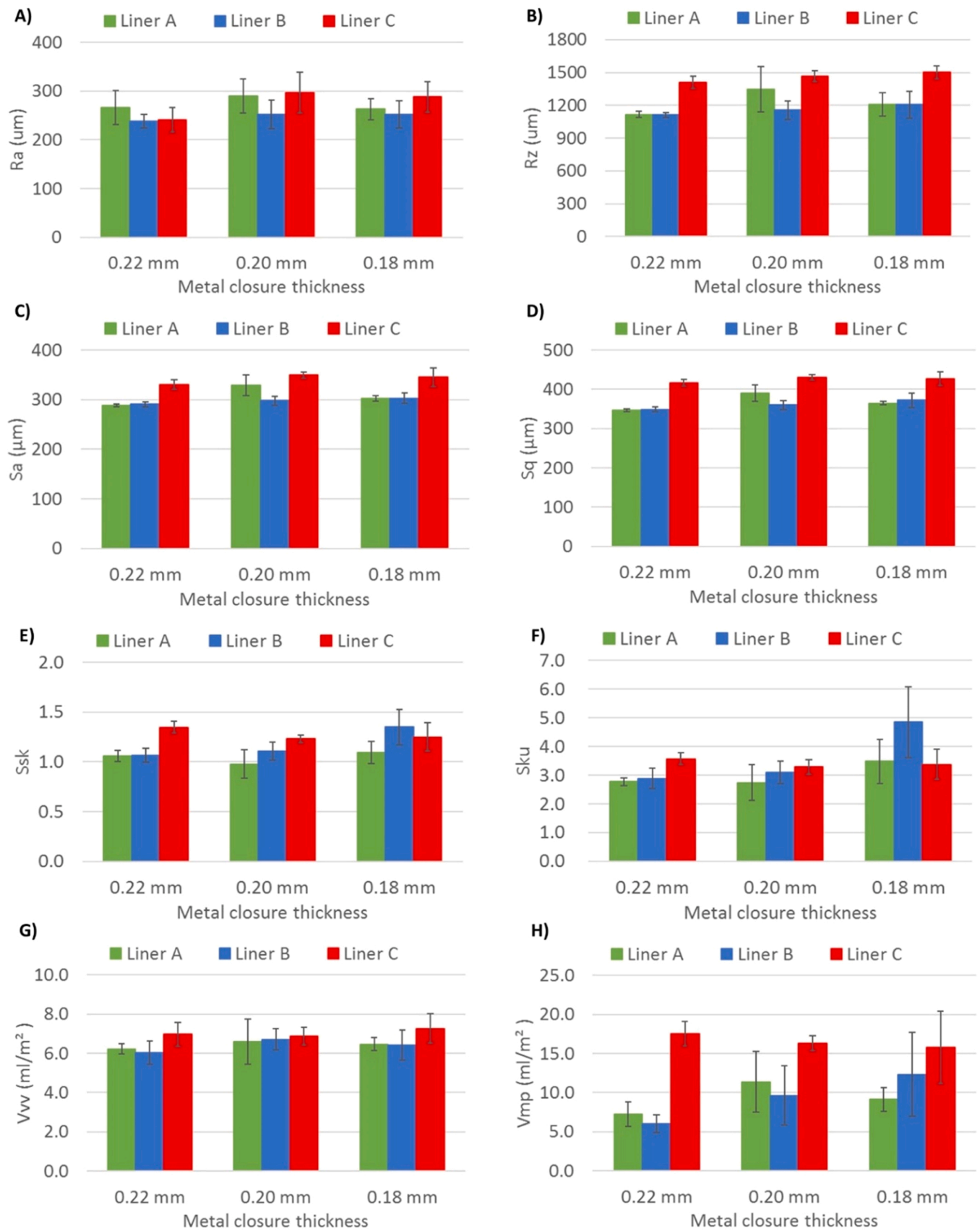
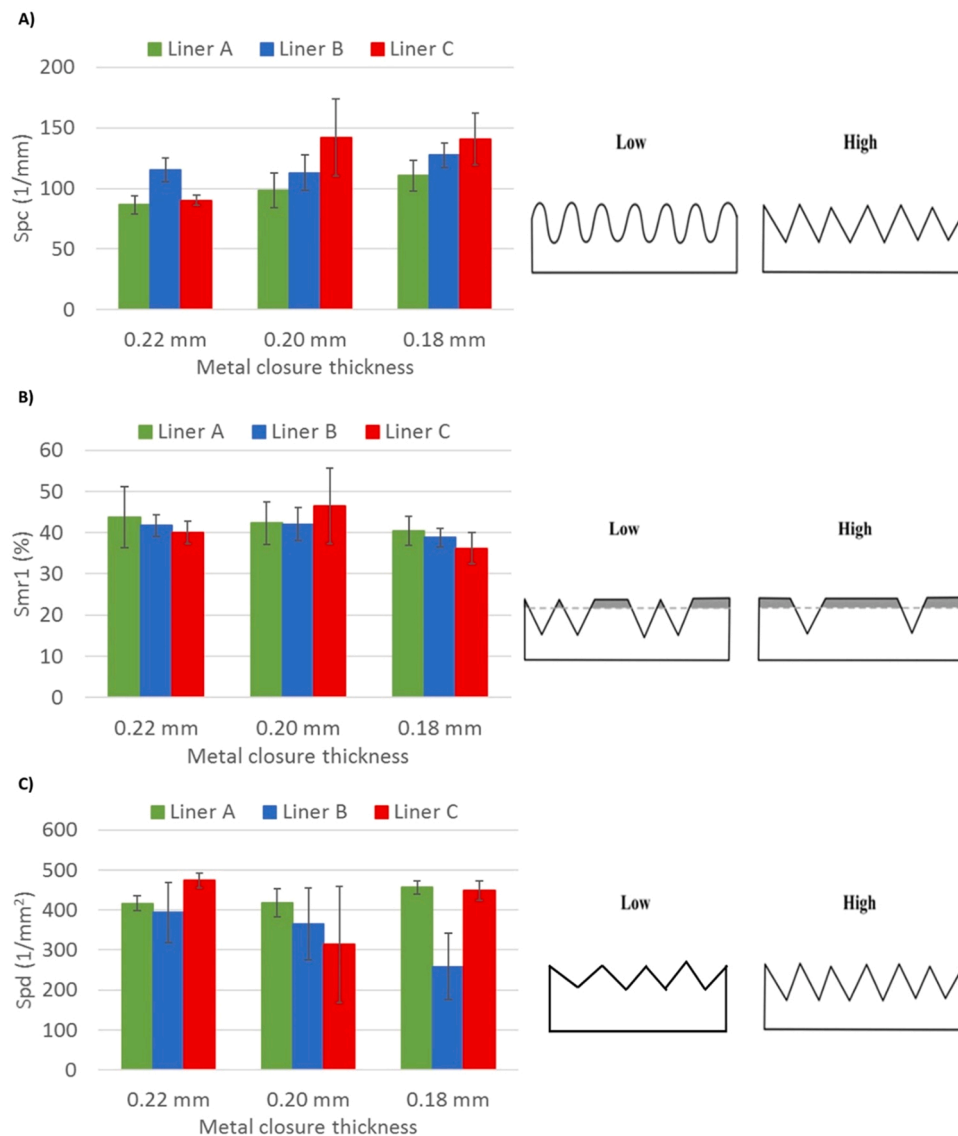


Fig. 5. (a) The height profile and (b) surface roughness,  $R_a$  as well as the roughness depth  $R_z$ , of the inner side of the metal cap shell as measured by the Keyence 3D profilometer VR-5000.





**Fig. 6.** Line and surface roughness parameters of different liners sealed in metal caps of a different thicknesses a)  $R_a$  (arithmetic mean surface roughness), b)  $R_z$  (surface roughness depth), c)  $S_a$  (arithmetical mean height), d)  $S_q$  (root mean square height), e)  $S_{sk}$  (skewness), f)  $S_{ku}$  (kurtosis), g)  $V_{vv}$  (average void volume), h)  $V_{mp}$  (peak material volume).



**Fig. 7.** The surface profile parameters of closure lips for different liners sealed in different thicknesses of metal caps a)  $S_{pc}$  (arithmetic mean peak curvature), b)  $S_{mr1}$  (peak material portion), c)  $S_{pd}$  (the density of surface peaks).

While  $R_a$  gives an average surface roughness,  $R_z$  can give information on for pore, hole or surface deformities detrimental to strength. Fig. 5 shows the height profile and surface roughness of the inner side of the bottle closure shell before the molten liner is applied. The 0.18 mm metal cap is equipped with a thinner metal sheet so it is mechanically weaker. A metal cap composed of a thinner sheet material might be less reliably press the sealing liner against the glass bottle mouth opening with the same force as a conventional body composed of thicker sheet material. Thus, the 0.18 mm metal cap is expected to cause an increased seal leakage. No significant difference was observed between surface roughness of different metal cap thicknesses; meaning no significant difference is expected for the adhesion of liner materials to the metal cap.

The results of line and surface roughness parameters of liner materials obtained from the 3D profilometer are shown in Fig. 6. No significant difference is observed in  $R_a$  values of different liner materials for the same metal closure thickness. However, metal thickness downsizing resulted in higher  $R_a$  values for Liner C (Fig. 6a) supporting the incremented leaking pressure of Liner C with metal thickness downsizing meaning increased seal leakage. Since leakage is a function of surface roughness for molded seals, a minimum leakage can be obtained when

the roughness is minimal (Widder, 2004). The difference between liner materials within the same metal closure thickness is observed in the  $R_z$  values. While the difference in  $R_z$  values of Liner A and B was not significant,  $R_z$  values of Liner C were significantly higher than those of Liner A and B (Fig. 6b). This finding supports higher seal leakage in Liner C than that of Liner A and B in the seal leaking pressure test results. Nevertheless, the  $R_a$  and  $R_z$  parameters provide only limited information about the real characteristics of a surface. For instance, these parameters are insufficient for providing any information about the height distribution, which were shown to be significant, particularly when estimating the number of direct contact patches as well as the effective contact area (Kozuch, Nomikos, Rahmani, Morris, & Rahnejat, 2018). The arithmetical mean height ( $S_a$ ) is the extension of  $R_a$  to a surface which is generally used to evaluate the surface roughness (Shi *et al.* 2019).  $S_a$  values also showed a similar trend to that of  $R_z$  values (Fig. 6c). The root mean square height ( $S_q$ ) value which is more sensitive to extreme surface peaks and valleys, shows the differences between the lining materials than  $S_a$  and  $R_z$  values better due to smaller standard deviations (Fig. 6d). The skewness value ( $S_{sk}$ ) represents the degree of symmetry of the surface heights around the mean plane. All  $S_{sk}$  results were positive ( $S_{sk} > 0$ ) indicating the predominance of peaks (Fig. 6e).

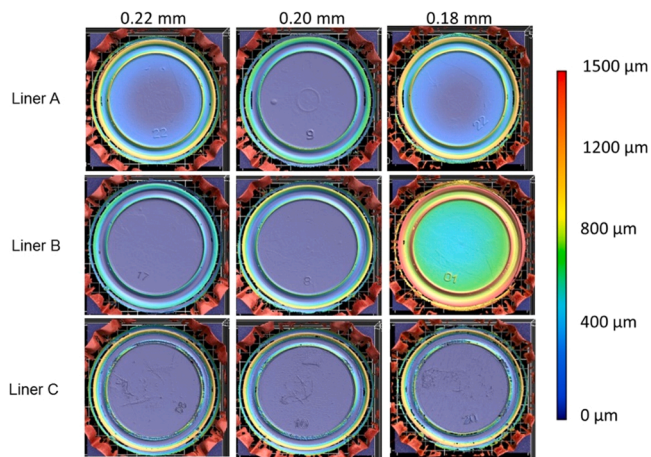


Fig. 8. The height profile of the liner materials after being sealed inside the metal cap shells of different thicknesses.

The kurtosis ( $S_{ku}$ ) is a measure of the peak sharpness. The combination of skewness and kurtosis permits identification of various defects on the surface (anomalous peaks or valleys). For a symmetrical Gaussian surface,  $S_{sk}$  is 0 and  $S_{ku}$  is 3 (Shi et al. 2019). Fig. 6f indicates that the surface of Liner C ( $S_{ku} > 3$ ) has always extreme peaks and metal thickness downsizing to 0.18 mm causes the presence of extremal peaks on the surface of Liner A and B, meaning locally higher stress levels. In theory,

seal leakage will decrease with an increase in the contact stress and contact width (Haruyama, Nurhadiyanto, Choiron, & Kaminishi, 2013). However, when these parameters are further increased, the actual contact area is reduced (Shi et al. 2019). When the actual contact area is too small, the contact stress will cause plastic deformation of the liner material, resulting in leakage.  $V_{vv}$  (average void volume) may provide information about the resulting void volume for fluid entrapment (Shi et al. 2019). No significant difference was observed for  $V_{vv}$  of liner materials due to metal downsizing. However, the average void volume  $V_{vv}$  of Liner C was higher than that of Liner A at 0.22 and 0.18 mm metal thickness (Fig. 6g). For sealing applications,  $V_{mp}$  (peak material volume) may provide insight into the amount of material available for seal engagement.  $V_{mp}$  of Liner C was significantly higher than that of Liner A and B at 0.22 mm metal cap thickness and didn't change significantly with metal thickness downsizing. However, there was a noticeable increase in  $V_{mp}$  values of Liner A and B with metal downsizing, meaning a better contact zone with the glass finish (Fig. 6h). Thus, for 0.18 mm thin metal caps with lower axial force, increases in the  $V_{mp}$  values may cause retention of leaking pressure of seals at the same level due to an increased contact area.

The result of surface profile parameters of closure lips obtained from the laser confocal microscope are shown in Fig. 7.  $S_{pc}$  (arithmetic mean peak curvature) represents that the curvature of the peaks are either rounded or pointed on the surface. It affects the degree of elastic and plastic deformation of a surface under loading. At 0.22 mm metal thickness, there was no significant difference between Liner A and Liner C. The lower value of  $S_{pc}$  compared to that of Liner B indicates that the

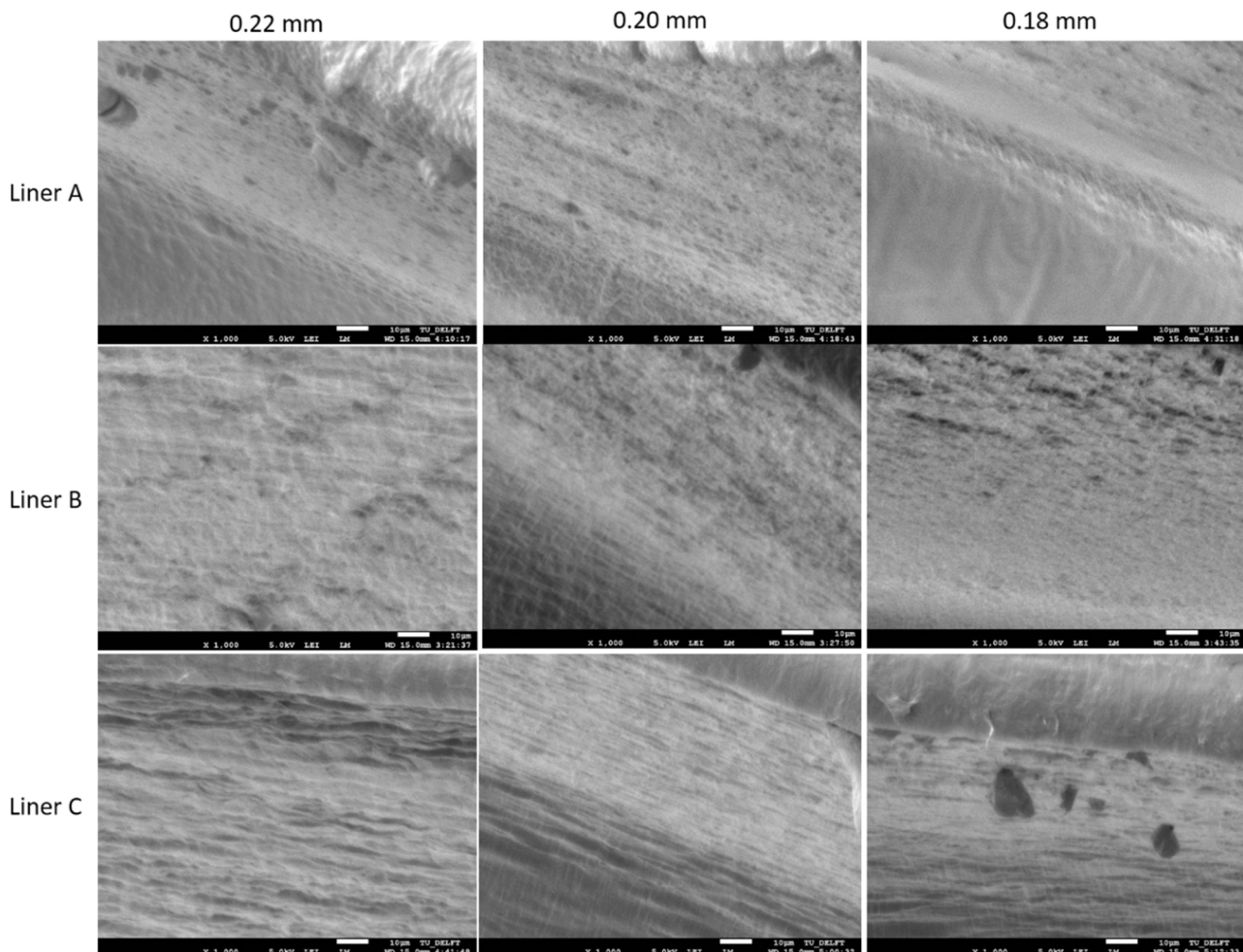
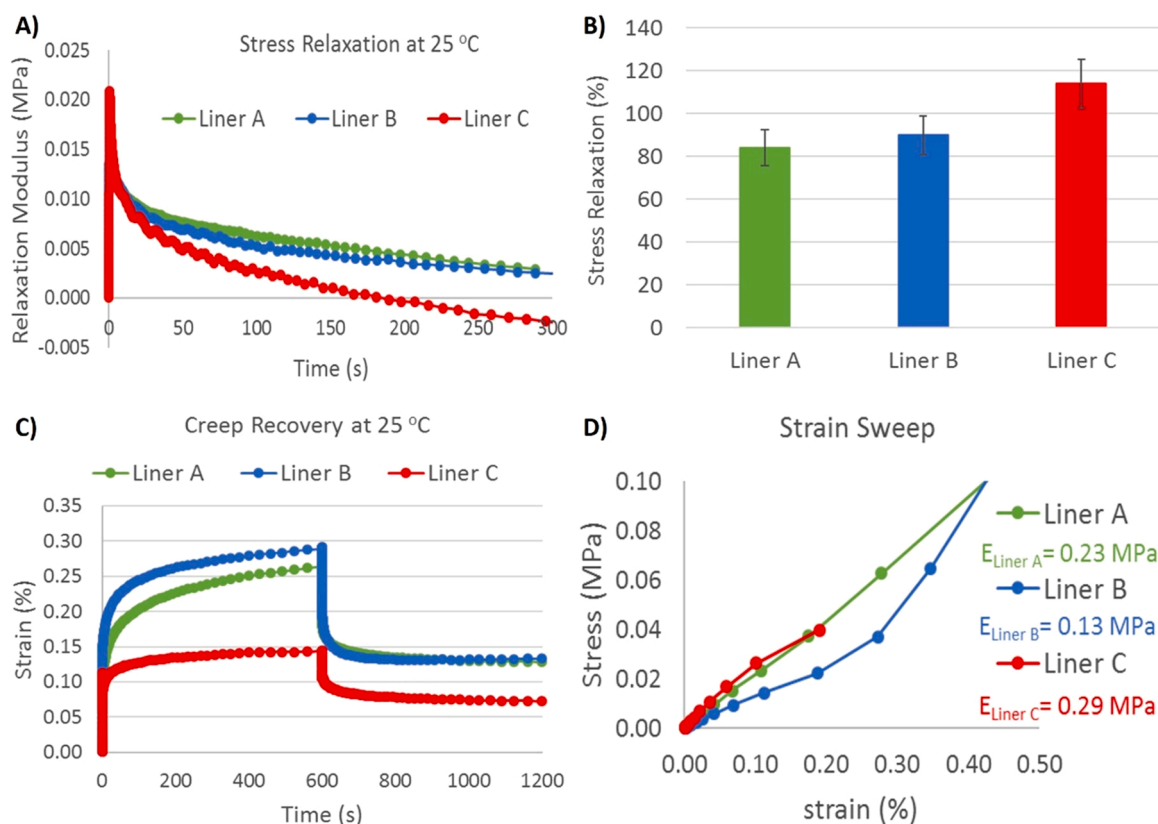


Fig. 9. The scanning electron microscopy (SEM) graphs of closure lips for different liners sealed into metal caps of different thicknesses.





**Fig. 10.** Stress relaxation and creep behavior results; a) relaxation modulus (MPa), b) stress relaxation (%), c) creep-recovery measurement results, d) strain sweep performed with a dynamic mechanical analyzer.

points of contact for Liner A and C show more rounded shapes and the observed incremental  $S_{pc}$  value with metal thickness downsizing indicates that Liner C possesses a more pointed shaped like surface (Fig. 7a). The peak material portion ( $S_{mr}$ ) is the percentage of material that comprises the peak structures and  $S_{mr1}$  (%) represents the areal material ratio that divides the reduced peaks from the core surface. There were no significant differences observed between the three liner materials (Fig. 7b), meaning the same amount of contact material at the sealing surface. The density of surface peaks ( $S_{pd}$ ) reflects the surface deformation on loading. A large number indicates more contact points with glass finish. The  $S_{pd}$  value of Liner A didn't change significantly with metal closure thickness. However, Liner B showed a gradual decrease of the average value, though hardly significant (Fig. 7c). Higher values of  $S_{pc}$  and  $S_{pd}$  would cause an increase in contact stresses, which leads as a result to larger deformations (Fehrenbacher, Hoerl, Bauer, & Haas, 2016). Fig. 8 shows the height profile of the liner materials as a representative of five different samples after molten liners had been applied to the inside of the bottle cap shell. The height of the liner materials on the closure lip ranges between 800 and 1100  $\mu\text{m}$ . Moreover, Liner C showed more voids on the lip surface than Liner A and B at 0.22 and 0.18 mm, which is supported by the data from Fig. 6g. It was noticed that the small surface roughness value  $R_a$  or  $R_z$  alone was not found to be a critical factor in the low leakage problem. Smaller values of  $S_{ktb}$ ,  $V_{vvs}$ ,  $S_{pc}$  and  $S_{pd}$  might play a more critical role on the leakage path patterns, resulting in a lower leakage rate by lowering liner deformation due to lower contact stress. Moreover, higher  $V_{mp}$  and  $S_{mr}$  values which are offering a better contact zone with the glass finish can also help decreasing the leakage rate.

Scanning electron microscopy (SEM) was used to study the surface morphology of the closure lips and SEM micrographs of the liner samples are presented in Fig. 9. Liner C sealed in a 0.22 mm thick metal cap

showed a more wrinkled surface morphology than that of Liner A and B. This finding is supported by the highest  $R_z$ ,  $S_a$  and  $S_q$  values of Liner C shown in Fig. 6. The observed cavities in Liner A sealed in the 0.22 mm thick metal cap can be attributed to its higher melt viscosities (respectively lower melt flow index–MFI shown in Table 1) with a longer molecular chain causing a higher resistance to fill the mold during compression. The SEM micrographs of liner materials sealed in the 0.20 mm thick metal caps show similar results. According to Fourier's law of heat of conduction, metal thickness is inversely proportional to the rate of heat transfer. Metal thickness downsizing to 0.20 mm can offer the advantage of improved thermal conductivity for good heat transfer and can eliminate the differences between material's viscosities. This can be also the reason for not observing cavities in Liner A sealed in the 0.18 mm thick metal cap. No differences were observed in micrographs of Liner B with metal thickness downsizing. However, Liner C sealed in the 0.18 mm metal caps showed cavities on the closure lip supported by a significantly decreased  $S_{mr1}$  (%) value of Liner C in Fig. 7.

The stress relaxation tests performed on the three batches of liners allowed for a direct comparison of their deforming behavior and the results are shown in Fig. 10. The results with less than 10% standard deviation in Fig. 10a indicate that the relaxation modulus decreases faster in Liner C. No significant difference is observed between stress relaxation behavior of Liner A and B. However, the relaxation of Liner C is significantly higher than that of the other two liners (Fig. 10b). This does seem to depend on chemical species in liner materials. For instance, Liner A and B consist of LDPE which has long chain branches compared with HDPE in Liner C. Since long chain branches are assumed to block reptation, rearrangement proceed slower (Graessley, 1982). This is why relaxation times in Liner A and B is longer. Moreover, the addition of SEBS in Liner A may decrease the relaxation rate possibly due to the increasing number of entanglement points, formation of physical

network and interactions between olefinic soft segments of SEBS and LDPE chains (Alanalp, Durmus, & Aydin, 2019). A considerable relaxation occurring in the Liner C material causes a large reduction of the sealing force in a practical application. This could possibly lead to a premature failure of the sealing system due to interfacial leakage (Ilseng, Skallerud, & Clausen, 2016). In Fig. 10c, Liner A and B show a large amount of creep under compression compared to Liner C. This finding is supported by the strain sweep data (static stress-strain curve) (Fig. 10d). As HDPE possess both higher crystallinity and density than LDPE, better creep resistance is noticeable in Liner C made with HDPE. The Young's modulus (measure of stiffness, elastic modulus) of liner materials was calculated from the slope of the linear portion of the stress-strain curve using the DMA. Moreover, the linear viscoelastic regime (LVR) was determined to measure stress relaxation and creep data accurately and reliably. A given uniaxial compressive stress creates more deformation in a material with low stiffness (Liner B: 0.13 MPa) than in one with a higher stiffness (Liner C: 0.29 MPa). In this case there was less leakage observed in Liner A and B in the practical application of the bottle sealing as a result of the metal thickness downsizing, because interstices caused by surface roughness are closed by the elastic deformations of the elastomer's surface. Materials which are relatively hard, like Liner C show low creep compliance. This allows for the onset of leakage to occur quickly due to poor sealing (Briscoe & Tweedale, 1989). It is also observed, that the average contact stress of the seal decreases with a shorter relaxation time which may result in an increase in the gas leakage rate of the seal. When the seal is compressed, the contact stress of the rubber seal is relaxed due to its own viscoelastic properties. The relationship between the leakage rate and the viscoelastic properties of the seal liner indicated that the gas leakage rate of the rubber seal increases as the contact stress decreases and the elastic modulus of the rubber seal increases (Dong, Ke, Zheng, Yang, & Yao, 2017). Moreover, the creep recovery compliance of Liner A is higher than that of Liner B, while creep compliance of Liner A is lower than that of Liner B due to its higher elastic modulus. Although Liner B is found to be a harder material than Liner A, Liner A shows to have a higher stiffness. The influence of creep recovery can be also seen from the value of compression set (Liner A: 17%, Liner B: 30%, Table 1) which represents the amount of residual deformation at a given time after release where 0% stands for full height recovery and no residual deformation and 100% for no recovery (Jau-nich, Stark, & Wolff, 2010).

It is important as spontaneous stress release of the seal is simulated that could occur during the seal application due to external forces or internal pressure variations. Recovery stress under compression is a manifestation of the entropy of the elastomer, and any change that reduces the entropy reduces the sealing capacity of a liner (Fisher, 1951).

#### 4. Conclusions

This paper discussed the effect of surface characteristics (roughness and form), stress relaxation and creep behavior in relation to the leakage rate of three different liner types by taking into consideration the metal closure thickness downsizing for improved sustainability and reduced costs. It was observed that sealing surface roughness and forms provide different stress levels on the gasket, affecting the leakage paths shape, size, and directions. Metal downsizing was possible with Liner A and B without a significant change in performance. However, the sealing performance of Liner C showed a significant decrease in performance. It was found that smaller values of not only the surface roughness value  $R_a$  or surface roughness depth  $R_z$  but also the surface height distribution

kurtosis  $S_{kt}$ , average void volume  $V_{nv}$ , arithmetic mean peak curvature  $S_{pc}$  and density of surface peaks  $S_{pd}$  played a critical role on the leakage path patterns, resulting in a lower leakage rate by lowering the liner deformation due to a lower contact stress. Moreover, higher peak material volume  $V_{mp}$  and peak material portion  $S_{mr}$  values offering a better contact zone with the glass finish can help decreasing the leakage rate.

The stress relaxation of Liner C was found to be the highest and the fastest which caused a large reduction of the sealing force and failure of the sealing system due to interfacial leakage. The elastic moduli of Liner A, B and C were found as 0.23 MPa, 0.13 MPa and 0.29 MPa, respectively. It was noted that the hardest Liner C showed the lowest creep compliance resulting in poor sealing performance as a result. For soft liners, the creep compliance of Liner A was lower than that of Liner B due to its higher elastic modulus. Moreover, creep recovery compliance of Liner A showed the highest compatibly with the lowest value of compression set. The sealing liner material must thus ensure sealing properties when thinner metal closures are used, primarily by means of the ratio of the seal surface contact pressure to the elastic modulus of the seal. Since the thinner metal closure has a lower surface contact pressure than the thicker one, the liner material should have a smaller elastic modulus to ensure the same sealing performance. We believe that apart from looking for the creep and relaxation performance of liners under static compression at room temperature and constant thickness, future research should also focus on the influence of temperature, as well as influence of liner thickness on relaxation and creep behavior in a more realistic setting.

#### Funding

This research was carried out under project number A17021b in the framework of the Research Program of the Materials innovation institute (M2i) ([www.m2i.nl](http://www.m2i.nl)) supported by the Dutch Government.

#### CRedit authorship contribution statement

**Deniz Turan:** Conceptualization, Methodology, Analysis and/or interpretation of data, Writing – original draft preparation; **Johannes A. Poulis:** Supervision, Writing – review & editing.

#### Acknowledgements

The authors very much appreciate the support for material supply by Actega DS GmbH. Authors also acknowledge HEINEKEN for discussions on problem definition. The authors would like to thank the following people Johan Bijleveld, Marlies Nijemeisland, Durga Mainali and Gertjan Mulder for training and making instruments available. All other laboratory staff: Fred Bosch, Victor Horbowiec, and the people from the TU Delft DEMO workshop.

#### Author contributions

The manuscript was written through contributions of all authors. All authors have given approval to the final version of the manuscript.

#### Appendix

See Table 1A

**Table 1A**  
Selected surface topography characterization parameters (Aver'Yanova et al., 2017).

Parameter	Explanation	Equation
S <sub>a</sub>	The mean height of the surface irregularities	$S_a = \frac{1}{L \times B} \iint_{00}^{LB} \eta(x,y) dx dy$
S <sub>q</sub>	The mean square deviation from the base plane is sensitive to extreme surface peaks and valleys	$S_q = \sqrt{\frac{1}{L \times B} \iint_{00}^{LB}  \eta^2(x,y)  dx dy}$
S <sub>sk</sub>	The skewness (asymmetry) of the height distribution is a measure of the asymmetry of the height discrepancies	$S_{sk} = \frac{1}{S_q^3 \times L \times B} \iint_{L \times B} \eta(x,y)^3 dx dy$
S <sub>ku</sub>	The kurtosis of the height distribution is a measure of the sharpness of its peaks	$S_{ku} = \frac{1}{S_q^4 \times L \times B} \iint_{L \times B} \eta(x,y)^4 dx dy$
S <sub>mr</sub>	The surface bearing area ratio characterizes the frictional and contact properties of the surface and also its wear resistance	$S_{mr(p)} = \frac{1}{L \times B} \iint_{\eta^*(x,y) < p} dx dy$
V <sub>mp</sub>	The material volume of the peaks permit assessment of the volume of material removed from the surface in wear	$V_{m(p)} = \frac{\iint_{\eta^*(x,y) > p} [\eta^*(x,y) - p] dx dy}{\iint_{L \times B} \left[ \eta^*(x,y) + \left  \frac{\min \eta(x,y)}{L \times B} \right  \right] dx dy}$
V <sub>vv</sub>	The average void volume in the surface valley region permits assessment of the fluid volume held in surface cavities	$V_{v(p)} = \frac{\iint_{\eta^*(x,y) < p} [p - \eta^*(x,y)] dx dy}{\iint_{L \times B} \left[ \frac{\max \eta(x,y)}{L \times B} - \eta^*(x,y) \right] dx dy}$
S <sub>pc</sub>	The mean peak curvature reflects the contact properties of the surface	$S_{pc} = -\frac{1}{2} \times \frac{1}{n} \sum_1^n \frac{\partial^2 \eta(x,y)}{\partial x^2} + \frac{\partial^2 \eta(x,y)}{\partial y^2}$
R <sub>a</sub>	The arithmetic average of the absolute values of the profile heights over the evaluation length	$R_a = \frac{1}{L} \int_0^L  \eta(x)  dx$
R <sub>z</sub>	The absolute vertical distance between the highest and lowest points of the profile within a sampling length	$R_z = \max(\eta(x)) + \min( \eta(x) )$

$\eta(x,y)$  is the deviation of the surface irregularities from the base plane; L, B are the length and width of the given section of surface corresponding to the baseline for the given type of surface irregularities.

**References**

Alanalp, M. B., Durmus, A., & Aydin, I. (2019). Quantifying effect of inorganic filler geometry on the structural, rheological and viscoelastic properties of polypropylene-based thermoplastic elastomers. *Journal of Polymer Research*, 26(2), 46.

Aver'Yanova, I., Bogomolov, D. Y., & Poroshin, V. (2017). ISO 25178 standard for three-dimensional parametric assessment of surface texture. *Russian Engineering Research*, 37(6), 513–516.

Briscoe, B., & Tweedale, P. (1989). The Influence of Debris Inclusion on the Performance of Polymeric Seals in Ball Valves. In *Tribology Series*, 14 pp. 259–265). Elsevier.

Dey, S., & Agrawal, M. K. (2016). Tinplate as a sustainable packaging material: recent innovation and developments to remain environment friendly and cost effective. *International Journal of Research in IT Management and Engineering*, 06(08), 9–22.

Dong, Y., Ke, Y., Zheng, Z., Yang, H., & Yao, X. (2017). Effect of stress relaxation on sealing performance of the fabric rubber seal. *Composites Science and Technology*, 151, 291–301.

Fehrenbacher, C., Hoerl, L., Bauer, F., & Haas, W. (2016). Description of the Pumping rate of shaft counterfaces in the sealing system radial lip seal using the 3D parameters of ISO 25178. *Tribology Online*, 11(2), 69–74.

Fisher, H. L. (1951). *Elastomers. Industrial & Engineering Chemistry*, 43(10), 2227–2235. DOI:2210.1021/ie50502a50020.

Gagula, G., Mastanjević, K., Mastanjević, K., Krstanović, V., Horvat, D., & Magdić, D. (2020). The influence of packaging material on volatile compounds of pale lager beer. *Food Packaging and Shelf Life*, 24, Article 100496.

Graessley, W. W. (1982). Effect of long branches on the temperature dependence of viscoelastic properties in polymer melts. *Macromolecules*, 15(4), 1164–1167.

Grelle, T., Wolff, D., & Jaunich, M. (2017). Leakage behaviour of elastomer seals under dynamic unloading conditions at low temperatures. *Polymer Testing*, 58, 219–226.

Haruyama, S., Nurhadiyanto, D., Choiron, M. A., & Kaminishi, K. (2013). Influence of surface roughness on leakage of new metal gasket. *International Journal of Pressure Vessels and Piping*, 111, 146–154.

Ilseng, A., Skallerud, B. H., & Clausen, A. H. (2016). Tension behaviour of HNBR and FKM elastomers for a wide range of temperatures. *Polymer Testing*, 49, 128–136.

Jaunich, M., Stark, W., & Wolff, D. (2010). A new method to evaluate the low temperature function of rubber sealing materials. *Polymer Testing*, 29(7), 815–823.

Koyama, M., Oda, Y., Kikuchi, H., & Yamada, M. (1996). Container closure with liner and method of producing the same. *U. S. Patent*, 542(5), 557.

Kozuch, E., Nomikos, P., Rahmani, R., Morris, N., & Rahnejat, H. (2018). Effect of shaft surface roughness on the performance of radial lip seals. *Lubricants*, 6(4), 99.

Moriga, T., Aoyama, N., & Tanaka, K. (2015). Development of a polyurethane sealing gasket with excellent sealing and opening properties. *Polymer Journal*, 47(5), 400–407.

Otsuka, M., Okamura, T., Suetsugu, N., Ohta, T., & Ono, S. (2003). A new concept of static rubber gasket for sealing rough surface. *SAE transactions*, 205–210.

Paternoster, A., Van Camp, J., Vanlanduit, S., Weeren, A., Springael, J., & Braet, J. (2017). The performance of beer packaging: Vibration damping and thermal insulation. *Food Packaging and Shelf Life*, 11, 91–97.

Robertson, G. L. (2016). *Food Packaging: Principles and Practice*. Boca Raton, FL: CRC press.

Sanchez-Gonzalez, M., & Pérez-Terrazas, D. (2018). Assessing the percentage of cork that a stopper should have from a mechanical perspective. *Food Packaging and Shelf Life*, 18, 212–220.

Shi, R., Wang, B., Yan, Z., Wang, Z., & Dong, L. (2019). Effect of surface topography parameters on friction and wear of random rough SURFace. *Materials*, 12(17), 2762.

Szymanski, A. (2011). Crown cork. Google Patents, WO2012074421A1.

Widder, E. (2004). Gaskets: surface finish effects in static sealing. In ASME B46 Seminar.